

Received:  
24 June 2016Revised:  
13 October 2016Accepted:  
3 January 2017<https://doi.org/10.1259/bjr.20160567>

Cite this article as:

Ghekiere O, Salgado R, Buls N, Leiner T, Mancini I, Vanhoenacker P, et al. Image quality in coronary CT angiography: challenges and technical solutions. *Br J Radiol* 2017; **90**: 20160567.

## REVIEW ARTICLE

# Image quality in coronary CT angiography: challenges and technical solutions

<sup>1,2,3</sup>OLIVIER GHEKIERE, MD, <sup>4</sup>RODRIGO SALGADO, MD, <sup>5</sup>NICO BULS, PhD, <sup>6</sup>TIM LEINER, MD, PhD, <sup>1</sup>ISABELLE MANCINI, MSc, <sup>7</sup>PIET VANHOENACKER, MD, PhD, <sup>8</sup>PAUL DENDALE, MD, PhD and <sup>9</sup>ALAIN NCHIMI, MD, PhD

<sup>1</sup>Department of Radiology, Centre Hospitalier Chrétien (CHC), Liège, Belgium

<sup>2</sup>Department of Radiology, Jessa Ziekenhuis, Hasselt, Belgium

<sup>3</sup>Faculty of Medicine and Life Sciences, Hasselt University, Hasselt, Belgium

<sup>4</sup>Department of Radiology, Antwerp University Hospital (UZA), Edegem, Belgium

<sup>5</sup>Department of Radiology, UZ Brussel, Brussels, Belgium

<sup>6</sup>Department of Radiology, Utrecht University Medical Center, Utrecht, Netherlands

<sup>7</sup>Department of Radiology, OLV Ziekenhuis Aalst, Aalst, Belgium

<sup>8</sup>Heart Center Hasselt, Jessa Ziekenhuis, Hasselt, Belgium

<sup>9</sup>GIGA Cardiovascular Sciences, Liège University (ULg), Domaine Universitaire du Sart Tilman, Rue de l'hôpital, Liège, Belgium

Address correspondence to: Dr Olivier Ghekiere

E-mail: [olivierghekiere@gmail.com](mailto:olivierghekiere@gmail.com)

## ABSTRACT

Multidetector CT angiography (CTA) has become a widely accepted examination for non-invasive evaluation of the heart and coronary arteries. Despite its ongoing success and worldwide clinical implementation, it remains an often-challenging procedure in which image quality, and hence diagnostic value, is determined by both technical and patient-related factors. Thorough knowledge of these factors is important to obtain high-quality examinations. In this review, we discuss several key elements that may adversely affect coronary CTA image quality as well as potential measures that can be taken to mitigate their impact. In addition, several recent vendor-specific advances and future directions to improve image quality are discussed.

## INTRODUCTION

The high negative-predictive value of coronary CT angiography (CTA) makes it a suitable tool for excluding significant coronary artery disease.<sup>1</sup> Coronary CTA is technically complex and places a greater emphasis on scanning technologies than any other type of CT examination. Indeed, coronary arteries both have small calibre and varying degrees of motion during the cardiac cycle.<sup>2</sup> Image quality can be degraded by many patient- and technique-related factors. Image artefacts are causes for misinterpretation, making the diagnostic accuracy of coronary CTA to a great extent dependent on their recognition and operator-awareness.<sup>2,3</sup> Potential problems related to these artefacts include insufficient tissue contrast, limited spatial and temporal resolution and inadequate volume coverage. The aim of this review was to discuss these technical issues, important recent vendor-specific solutions as well as future directions.

## IMAGE QUALITY IN CORONARY CT ANGIOGRAPHY

The basic principle of coronary CTA is to acquire a motion-free volumetric data set through the heart during peak

coronary artery enhancement. The final image quality and associated radiation exposure are determined by both technical and patient-related factors. Image quality is therefore a complex entity for which there is no single objective scale. It has been recently established that coronary artery size is an important parameter in determining image quality.<sup>4</sup> While spatial resolution, as discussed in the next paragraph, is the only objective method to evaluate image detail, other factors have been discussed in the literature. In practice, the final end point of all factors influencing coronary CTA image quality is their impact on image interpretation, which assumes that all of the following quantitative or qualitative variable scaling should be within an "acceptable" range: noise, vascular enhancement and coronary motion.

Image noise is one of the principal determinants of image quality, and it mainly depends on the number of X-ray photons reaching the detector. Image noise is influenced by technical and patient-related parameters (e.g. weight and anatomy), regardless of the filters used during the image reconstruction process to achieve the desired amount of

image sharpness vs noise. Image noise can be measured quantitatively by placing a region of interest (ROI) in contrast-enhanced structures (e.g. left ventricle cavity or thoracic aorta). The then obtained standard deviation of the Hounsfield unit values within the ROI area is a measure of image noise. Background noise can also be considered as the standard deviation of an ROI within the air (e.g. trachea or main bronchus).<sup>5</sup> Although no standard cut-off values of image noise have been reported, some authors suggested values of  $\leq 30$  HU for improved coronary CTA image quality.<sup>6-8</sup>

Besides image noise, image interpretability is further influenced by the degree of vascular enhancement. Previous reports have suggested that a vascular attenuation value of  $>400$  HU in the aorta is required for coronary CTA image interpretability.<sup>6-10</sup>

While vascular enhancement and image noise both are defining parameters in determining image quality, in practical terms it is more useful to use the signal-to-noise ratio. Signal-to-noise ratio is a generic term to indicate how much signal vs how much noise a particular image has. Similarly, contrast-to-noise ratio is determined by the differences in CT density values between different materials vs the background noise.

Table 1. Main coronary CT angiography artefacts causes and solutions

Artefacts	Problem	Cause	Solution
Blurring	Motion	<ul style="list-style-type: none"> <li>-HR &gt; acquisition speed</li> <li>-Respiration during acquisition</li> <li>-Inappropriate cardiac cycle phase reconstruction</li> </ul>	<ul style="list-style-type: none"> <li>-HR control (<math>\beta</math>- or calcium channel blockade, ivabradine)</li> <li>-Breath-hold instructions</li> <li>-Optimal cardiac cycle phase reconstruction</li> <li>-Use multisegment acquisition/reconstruction</li> <li>-Intelligent boundary detection</li> </ul>
Stairstep or banding	<ul style="list-style-type: none"> <li>-Motion</li> <li>-Cardiac cycle phase misregistration</li> </ul>	<ul style="list-style-type: none"> <li>-HR variation (tachycardia/arrhythmia)</li> <li>-ECG signal failure</li> <li>-Respiration during acquisition</li> </ul>	<ul style="list-style-type: none"> <li>-HR control (<math>\beta</math>- or calcium channel blockade, ivabradine)</li> <li>-Optimal cardiac cycle phase reconstruction</li> <li>-ECG editing</li> <li>-Pre-scan ECG quality check</li> <li>-Breath-hold instructions</li> </ul>
Streak	Dark bands through objects adjacent to high-attenuation structures (beam-hardening effect)	<ul style="list-style-type: none"> <li>-Metallic implants, surgical clips and coronary stents</li> <li>-Vessel filled with high iodine concentration</li> </ul>	<ul style="list-style-type: none"> <li>-Avoid undiluted contrast (use saline bolus flush)</li> <li>-Use a high-kilovoltage monoenergetic X-ray beam (dual-energy CT)</li> </ul>
Blooming	High-attenuation objects appear larger than they are	<ul style="list-style-type: none"> <li>-Coronary calcifications</li> <li>-Metallic implants, clips and coronary stents</li> </ul>	<ul style="list-style-type: none"> <li>-Use high spatial resolution reconstruction algorithms + iterative reconstruction (to decrease the noise)</li> <li>-Use the smallest available focal spot</li> <li>-Use a high kilovoltage monoenergetic X-ray beam (dual-energy CT)</li> </ul>
Windmill	Highly attenuating structures are surrounded by low-attenuating rims, and low attenuating structures appear larger and have a "fan-like" appearance	<ul style="list-style-type: none"> <li>-Moving structures during acquisition</li> <li>-HR &gt; temporal resolution &gt; spiral acquisition pitch</li> </ul>	<ul style="list-style-type: none"> <li>-Prefer sequential acquisition</li> <li>-HR control (<math>\beta</math>- or calcium channel blockade, ivabradine)</li> <li>-Optimize spiral scanning pitch</li> </ul>
Low attenuating	Air bubbles	<ul style="list-style-type: none"> <li>-Air within the contrast material bolus</li> <li>-Surgery</li> </ul>	Check i.v. line before contrast injection

ECG, electrocardiogram; HR, heart rate.

When image noise and vascular enhancement are adequate, the remaining interpretability factors are motion related. These are subjective by nature, evaluated visually as apparent blurring of the coronary artery contours and luminal visualization using Likert scales.<sup>4,11,12</sup>

## FACTORS AFFECTING IMAGE QUALITY

Technical parameters mainly include temporal resolution, spatial resolution, contrast resolution and radiation dose. It is further essential to synchronize image acquisition with cardiac motion by simultaneous electrocardiogram (ECG) recording. These technical factors are closely linked to each other in terms of balancing image quality vs radiation exposure.<sup>3,13</sup>

Temporal resolution is the minimal time necessary to compile all X-ray data that are required to calculate or reconstruct one cross-sectional CT data set. A high temporal resolution is required in coronary CTA to ensure motion-free image quality of the fast-moving coronary arteries. The most relevant parameter with a proportional impact on temporal resolution is the rotation speed of the gantry tube.

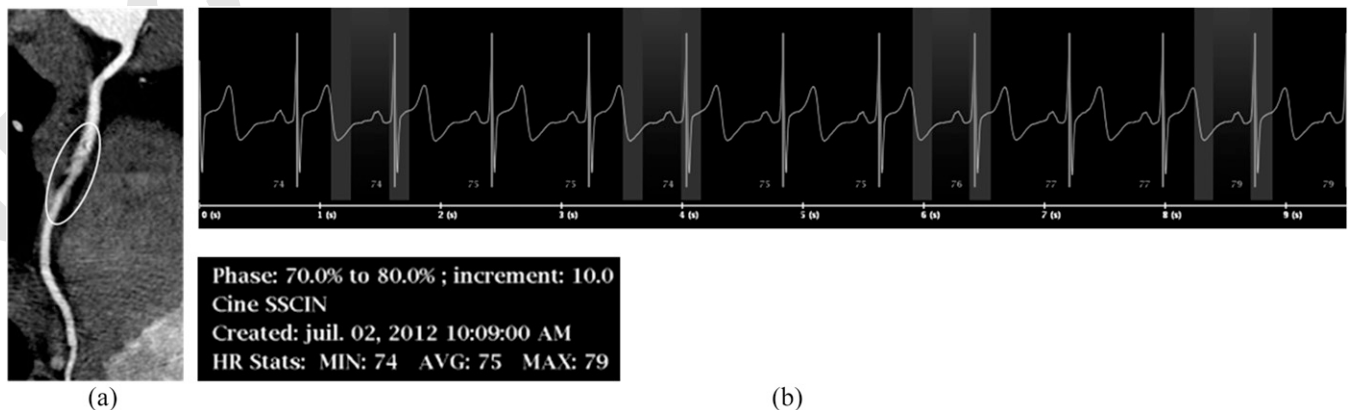
Spatial resolution defines the ability of a CT scanner to discern high-contrast anatomic details and is often specified in terms of

0 line pairs per centimetre obtained from phantom scans. It must  
 1 be considered both in the scan  $x$ - $y$  plane (in-plane) as well as in  
 2 the  $z$  direction (through-plane). Technically, the full width half  
 3 maximum (FWHM) of the point spread function expresses the  
 4 performance of CT scanners with regard to spatial resolution.  
 5 The FWHM defines whether two adjacent structures will be  
 6 represented separately in the images; two structures separated by  
 7 at least one FWHM can in general be distinguished from each  
 8 other, whereas two structures separated by  $<1$  FWHM are  
 9 bound to merge together in the reconstructed image. As such,  
 10 the spatial resolution depends on the detector properties, but  
 11 also on the reconstruction filter used, the object contrast and  
 12 image noise. Since this information is not available on images,  
 13 the voxel size is often used as an alternative surrogate marker.<sup>14</sup>

14  
 15 Voxel size depends on pixel size within the axial image and  
 16 through-plane resolution. It is determined by the matrix (e.g.  
 17  $512 \times 512$ ) and the field of view, whereas through-plane reso-  
 18 lution depends on the detector aperture width and focal spot  
 19 size. According to the Nyquist frequency equation, the minimal  
 20 coronary diameter evaluable without sampling error should be  
 21 at least the double of the voxel size.<sup>3</sup> An intrinsic spatial reso-  
 22 lution (expressed as FWHM) of about 0.5–0.7 mm, a voxel size  
 23 of about  $0.5 \times 0.5 \times 0.5$  mm or smaller are, in general, adequate  
 24 to image most of the coronary arteries.

25  
 26 Fast coverage of the entire heart using the shortest acquisition  
 27 time helps to avoid breathing-related artefacts, which can be  
 28 achieved by increasing detector size and therefore anatomic cov-  
 29 erage per rotation. In current multidetector CT scanners, detector  
 30 arrays ( $N \times T$ ) range from about 40 mm to 160 mm, where  $T$  is  
 31 the individual slice thickness and  $N$  is the number of simulta-  
 32 neously acquired slices. When the whole heart is within the an-  
 33 atomic detector coverage per rotation, no table movement is  
 34 necessary. Otherwise, a varying amount of table movements and  
 35 number of heart cycles is necessary to ensure complete cardiac  
 36 coverage. The associated pitch is defined as the ratio of table feed  
 37 per rotation to the detector coverage;  $p = \text{table feed}/(N \times T)$ , with  
 38 typical values in CCTA ranging from 0.2 to 0.4 with single X-ray  
 39 tube scanners, and up to 3 with dual-source CT (DSCT).<sup>13</sup>

40  
 41  
 42 Figure 1. Long-axis curvilinear reformation of the right coronary artery on a prospective electrocardiogram (ECG)-triggered  
 43 coronary CT angiography scan shows cardiac motion-related blurring artefact of the second segment (a, circle), due to a high heart  
 44 rate (HR), as shown on the simultaneously recorded ECG (b, average HR = 75 bpm).



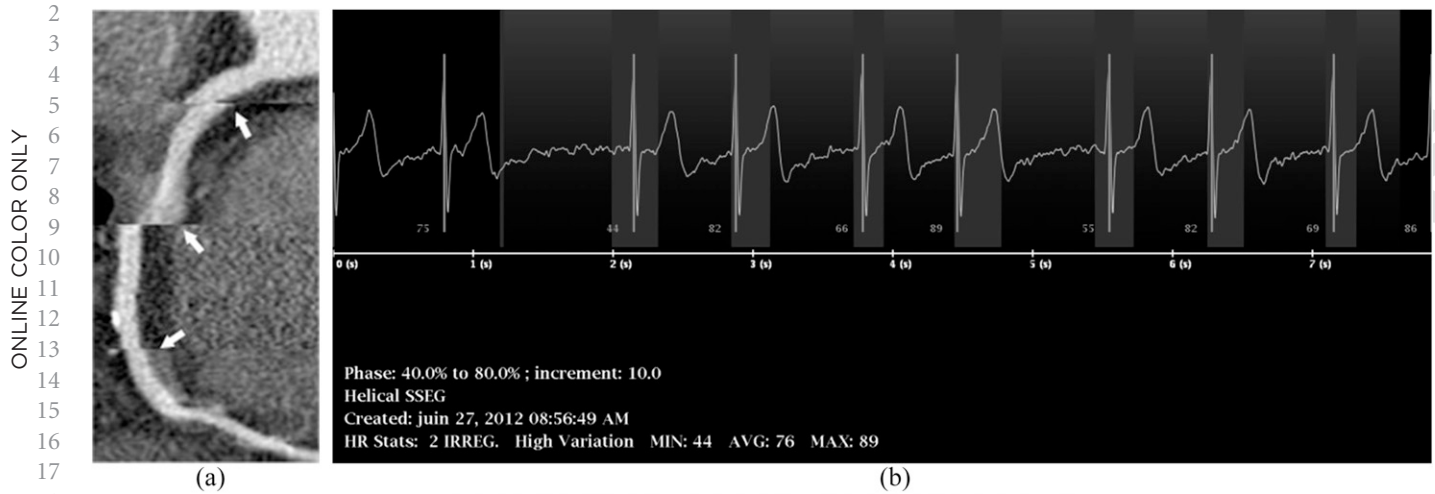
59 The often used term “contrast resolution” refers to the smallest  
 60 difference in material density that can be detected between ad-  
 61 jacent objects; it is often described as percentage (%) density  
 62 difference at a defined exposure level.

63  
 64 Radiation exposure can be quantitatively assessed by standard  
 65 technical dose descriptors: the volume CT dose index (in milligray  
 66 and dose-length product (in milligray centimetre). The  
 67 estimated effective dose ( $E$ ; in millisievert) represents the bi-  
 68 ological risk by the whole-body dose to a reference human. It is  
 69 preferably estimated by using a detailed computational organ  
 70 dose model that accounts for selected techniques, anatomical  
 71 location of the scan and patient size.<sup>15,16</sup> For practical reasons,  
 72 a rough estimate can also be provided by using a general  
 73 dose-length product to  $E$  conversion coefficient, the so-called  
 74  $k$ -factors that are determined by the anatomical location. The  
 75 reported use of conversion factors that are established for con-  
 76 ventional chest CT  $k = 0.014$ – $0.017$  mSv mGy<sup>-1</sup> cm<sup>-1</sup> tend to  
 77 severely underestimate the  $E$  in coronary CTA, where a value of  
 78  $k = 0.026$  mSv mGy<sup>-1</sup> cm<sup>-1</sup> is more appropriate.<sup>15</sup> The estima-  
 79 tion of  $E$  remains problematic for partial-body exposure, with an  
 80 inherent relative uncertainty of approximately  $\pm 40\%$ .<sup>17</sup> There-  
 81 fore, the exact impact of dose-reducing strategies should be  
 82 evaluated by using technical dose descriptors. Nevertheless,  $E$   
 83 remains valuable to compare dose between anatomic regions  
 84 and with other imaging modalities. Radiation dose is closely  
 85 related to image quality, and both are influenced by virtually all  
 86 patient-specific and CT acquisition parameters, including tube  
 87 current (milliamperere), energy (kilovoltage), gantry rotation  
 88 speed, scanning length and table speed.<sup>17</sup>

### IMAGE QUALITY FAILURE AND ARTEFACTS

90 Image artefacts usually result from the failure of previously men-  
 91 tioned determinants of image quality. Clinically relevant artefacts  
 92 on CCTA and their potential solutions are summarized in Table 1.  
 93 The most common artefacts are related to cardiac, pulmonary or  
 94 bulk body motion, resulting in coronary artery blurring (Figure 1)  
 95 and stairstep artefacts (Figure 2). Their presence depends on the  
 96 scanner temporal resolution, but also on the presence of extrac-  
 97 ardiac movement such as respiratory or voluntary motion.

0 Figure 2. Long-axis curvilinear reformation of the right coronary artery on retrospective electrocardiogram (ECG)-gated coronary 59  
 1 CT angiography shows stairstep artefacts (a, arrows) due to cardiac arrhythmia, as shown on the simultaneously recorded ECG (b). 60

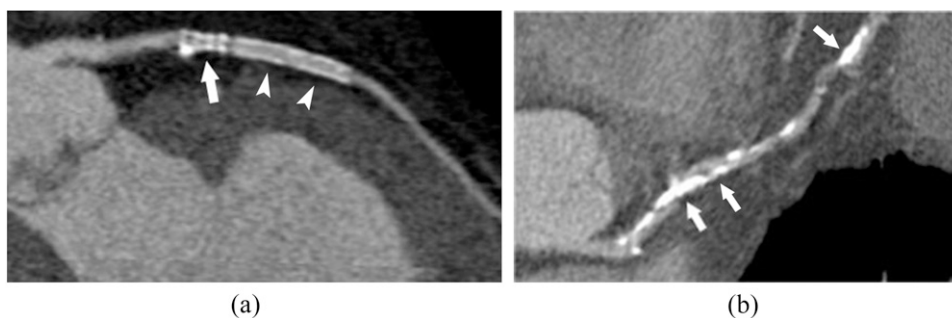


20 Blurring occurs when the temporal resolution is insufficient to  
 21 accurately register the moving targeted structure [e.g. when data  
 22 sampling exceeds the diastolic rest period, either due to a high  
 23 heart rate (HR), or due to the selection of an inappropriate  
 24 reconstruction window]. The right coronary artery is most  
 25 commonly affected owing to its higher velocity and range of  
 26 motion compared with other coronary segments.<sup>2</sup>

28 Banding or stairstep artefacts are section gaps in imaging data  
 29 due to cardiac phase misregistrations between consecutive gan-  
 30 try rotations. The most frequent causes are arrhythmia or HR  
 31 variation during acquisition.

33 Beam hardening is caused by an increase in mean photon energy  
 34 of the X-ray beam when it passes through a cross-section with  
 35 heterogeneous density. The lower energy photons of the poly-  
 36 chromatic beam are primarily absorbed, resulting in a higher  
 37 mean energy of the beam when it reaches the detector. It results  
 38 in dark bands throughout the image, the so-called streak arte-  
 39 facts. In practice, these artefacts are typically generated by highly  
 40 attenuating structures or interfaces such as high iodine con-  
 41 centration (e.g. in the superior vena cava), surgical clips and  
 42 metallic implants (pacemaker, stent struts).

44 Figure 3. High-attenuating coronary CT angiography artefacts on long-axis curvilinear reformation images of the left anterior 103  
 45 descending artery: (a) a 65-year-old male with history of multiple coronary stentings. Two stents are visible, with the proximal one 104  
 46 being highly attenuating (arrow) and preventing lumen visualization, while the distal stent exhibits a better luminal visibility 105  
 47 (arrowheads). (b) A 69-year-old male with diabetes mellitus. Extensive calcifications prevent luminal assessment (arrows). 106

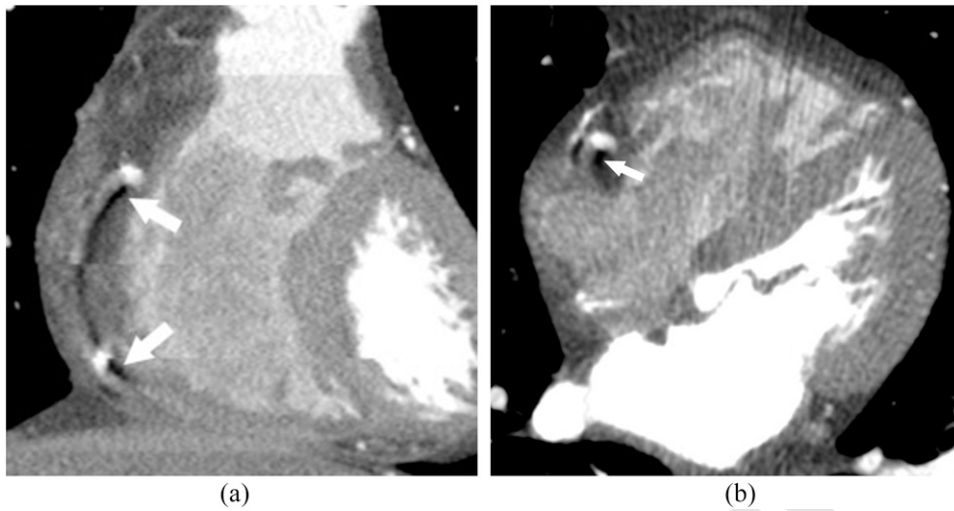


5 In blooming artefacts, high-attenuation objects appear larger  
 6 than they are. This results from multiple factors, including in-  
 7 adequate photon energy and partial volume effect; the latter is  
 8 caused by an insufficient temporal and spatial resolution par-  
 9 ticularly in the z direction.<sup>13</sup> Coronary stents, and to some ex-  
 10 tent vascular calcifications, are of special importance for  
 11 attenuation-related effects, as they generate both streak and  
 12 blooming artefacts, causing inappropriate vessel lumen visibility  
 13 or in-stent visualization due to motion, partial volume effect and  
 14 beam hardening (Figure 3).

16 Blooming artefact magnitude and stent lumen visibility largely  
 17 depend on stent size, strut thickness, material and mesh de-  
 18 sign.<sup>18</sup> Magnesium stents are far more favourable for coronary  
 19 CTA than tantalum-coated stents with up to 90% in-stent visi-  
 20 bility, depending on stent size.<sup>19</sup>

22 Helical artefacts with their typical windmill-like appearance  
 23 are seen in moving objects during spiral acquisition, or in  
 24 cases with ECG synchronization failure. The table movement  
 25 during the acquisition results in projections from slightly  
 26 different parts of the object. In coronary artery segments  
 27 that are obliquely oriented along the z-axis, this spiral

0 Figure 4. Coronal (a) and axial (b) reformats of coronary CT angiography shows low-density artefacts (arrows) around the contrast- 59  
 1 filled right coronary artery, due to inadequate spiral pitch with regard to heart rate. 60



21 interpolation process results in hypodense areas surrounding 22  
 23 the vessels (Figure 4).

24 Finally, image artefacts can also theoretically be caused by low- 25  
 26 attenuating objects such as air bubbles introduced in the right 27  
 28 heart or pulmonary artery during contrast material adminis- 29  
 30 tration or in the mediastinum after surgery.<sup>2,3</sup> In practice, the

hypodense zones surrounding these air bubbles do not alter 80  
 81 coronary visibility.

82 **IMAGE QUALITY IMPROVEMENT STRATEGIES**

83 All the major CT scanner vendors have devised their own pro- 84  
 85 prietary solutions for approaching the key artefacts and technical 86  
 87 limitations discussed above (Figure 5 and Table 2).

31 Figure 5. Major changes in coronary CT angiography technology over the first decade of the 21st century: while the number of 88  
 89 detectors and the coverage have been increased more than 10-fold, the gantry rotation time has been decreased by more 90  
 91 than a half. 92

32  
33  
34  
35  
36  
37  
38  
39  
40  
41  
42  
43  
44  
45  
46  
47  
48  
49  
50  
51  
52  
53  
54  
55  
56  
57  
58

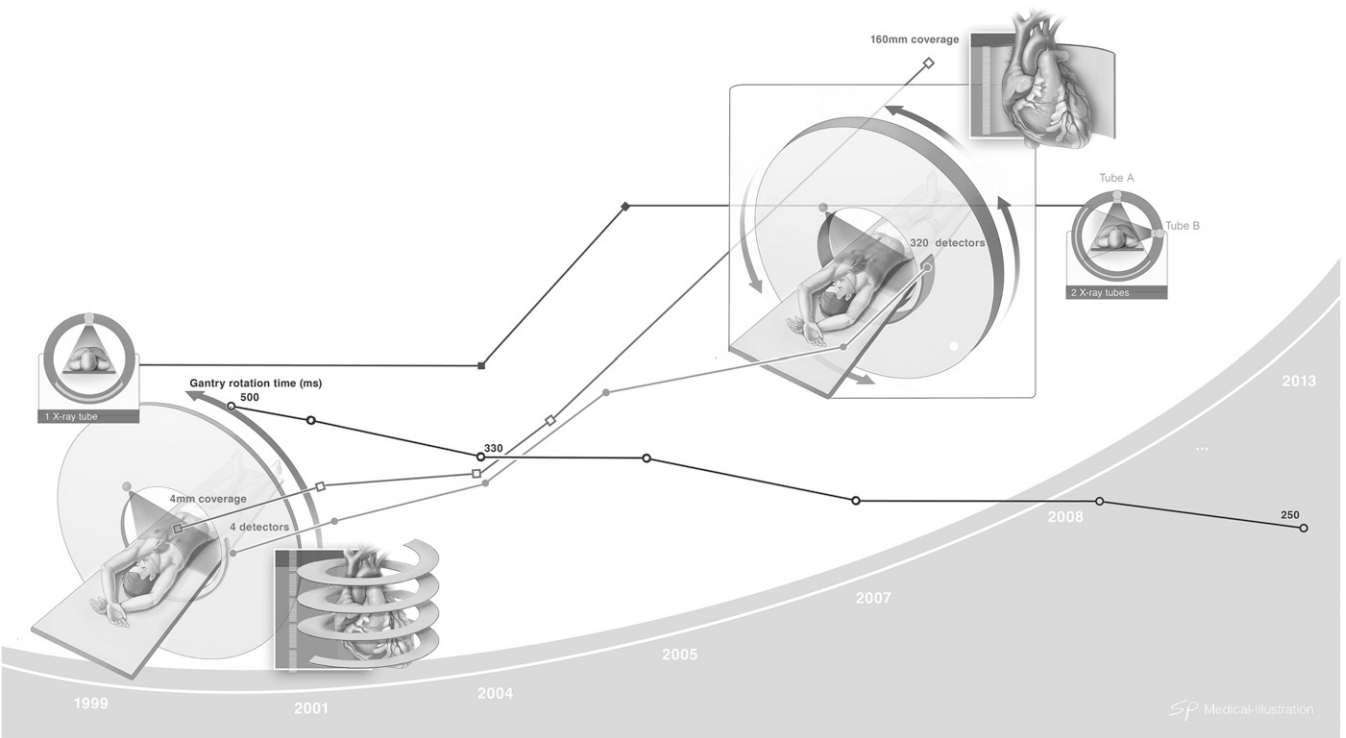


Table 2. Top four vendor recent technological advances in coronary CT angiography

Item	Vendor			
	General electric	Philips	Siemens	Toshiba
Arrhythmia	–Adaptative gating –ECG R-peak Editor	–Autoarrhythmia detection –ECG R-peak Editor	–Adaptive cardio sequence –ECG R-peak Editor	–Arrhythmia detection –ECG R-peak Editor
Gantry rotation speed (ms)	280	270	250	275
Maximum z-axis coverage/rotation (sequential) (cm)	16	8	7.68	16
Number of X-ray tubes	1	1	1 or 2	1
Current detector technology	Gemstone clarity	NanoPanel prism (IQon)	Stellar <sup>infinity</sup>	PURE <sup>V</sup> ision
Hybrid noise reduction software acronym	ASIR	iDose4	IRIS SAFIRE ADMIRE	AIDR AIDR 3D
Full noise reduction software acronym	MBIR or Veo	IMR		FIRST forward projected MBIR solution

3D, three-dimensional; ADMIRE, advanced modelled iterative reconstruction; AIDR, adaptive iterative dose reduction; ASIR, adaptive statistical iterative reconstruction; ECG, electrocardiogram; iDose4, i-dose iterative reconstruction; IMR, iterative model-based reconstruction; IRIS, iterative reconstructions in image space; MBIR, model-based iterative reconstruction; SAFIRE, sinogram affirmed iterative reconstruction.

Besides the discussed technical parameters, a successful coronary CTA also depends on proper patient selection and preparation (Figure 6). Furthermore, as with every CTA examination, a strong and homogeneous arterial enhancement of the coronary arteries is required. Important parameters to consider here include contrast agent volume, iodine concentration, injection speed and bolus duration, which should be adjusted to the body habitus of the patient [e.g. body mass index (BMI)].<sup>20</sup> Intraluminal contrast attenuation, a determinant of image quality, is also influenced by other technical parameters,<sup>21</sup> as for e.g. it has been showed that lowering the kilovoltage from 120 kV to 100 kV not only reduces radiation exposure, but also results in a significant increase (27–36%) of the vascular attenuation at the same injection rate. This is due to the higher attenuation of iodine at lower energy.<sup>22,23</sup> However, image noise is also increased in the range of 16–81%,<sup>22,24</sup> which allows further decrease of the tube energy to 80 kV only in children and adults with low BMI.<sup>21,25</sup> A more extensive discussion falls outside the scope of this review.

#### Patient selection and preparation

Patients with heavily calcified coronary arteries are subject to a higher rate of false-positive examinations, owing mainly to streak and blooming artefacts generated by these high-density structures.<sup>26,27</sup> Even with 64-slice and newer CT systems, the sensitivity and specificity of coronary CTA for significant stenosis remains high in the presence of severe calcifications.<sup>28</sup> Because motion further intensifies calcium-related artefacts,<sup>26</sup> patients should be screened for compliance to breath-hold and HR stability. Depending on the temporal resolution of the scanner, patients with irregular HR or HR above a certain limit (typically 65 beats per minute) are pre-medicated with beta-

blockers in some facilities, both to improve image quality and to reduce radiation exposure. However, the efficacy of beta-blocker administration to consequently achieve the targeted HR remains a subject of discussion.<sup>29</sup> In patients with relative or absolute contraindications to beta-blocker administration, calcium-channel blockers and ivabradine are known alternatives.<sup>30</sup>

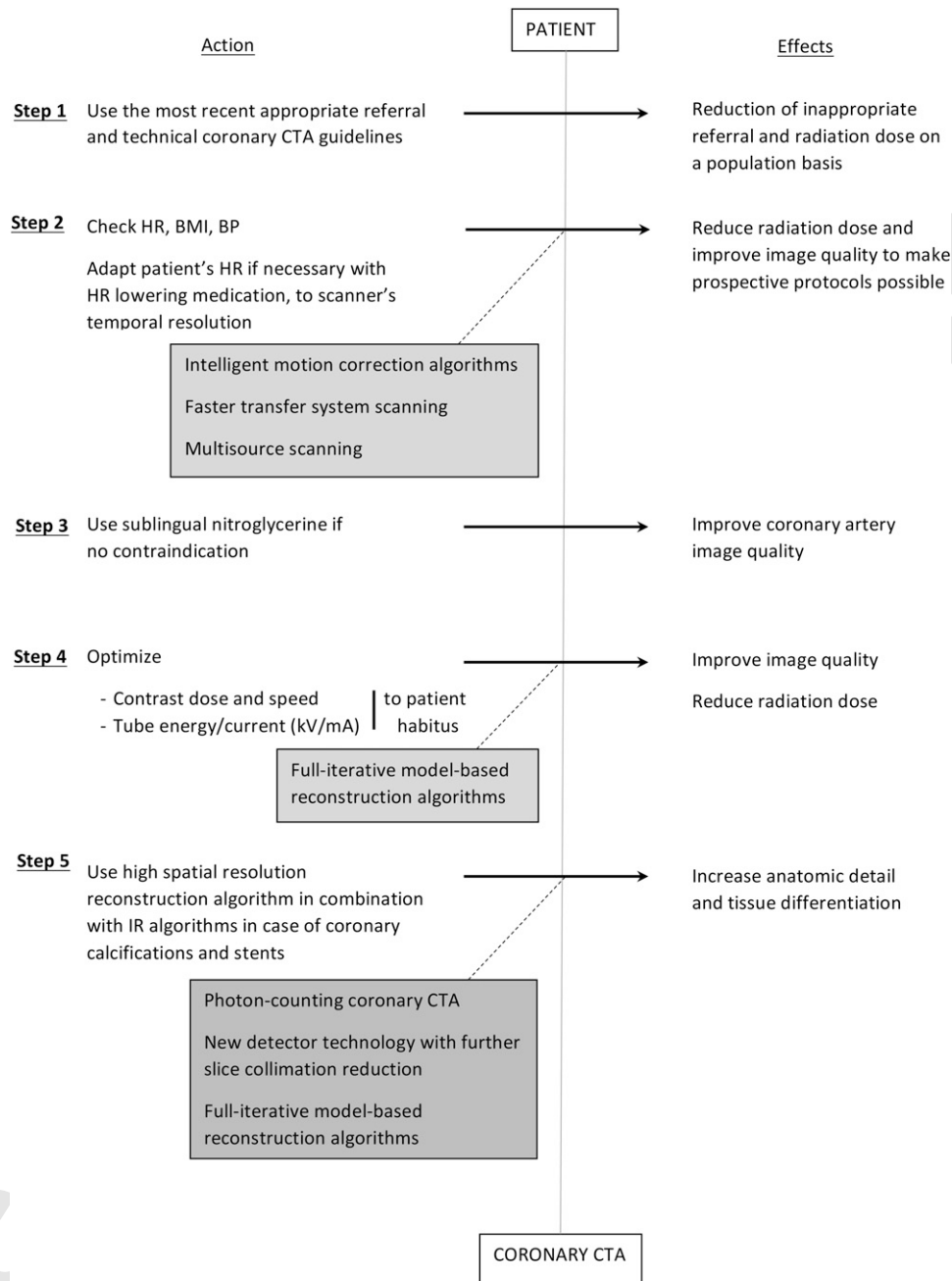
Finally, the administration of 0.4-mg sublingual nitroglycerin prior to coronary CTA increases the coronary diameter for improved image quality, especially for smaller branches.<sup>31</sup>

#### Hardware solutions

Significant advances have taken place during the past decade for the main scanner hardware component, the gantry, containing the tube(s) and detectors. All vendors have placed a critical emphasis on the improvement of the gantry rotation speed and (varying across vendors) the increase of number of detectors, as such improving the data acquisition.<sup>12,32</sup> Scan duration should be as short as possible to limit motion artefacts of the fast-moving coronary arteries.

In coronary CTA, partial reconstruction algorithms allow image reconstruction from data acquired within a half gantry rotation, the so-called half-scan.<sup>3</sup> This may be confusing, since the X-ray fan beam angle of the CT detectors (approximately 50°) plus a transition angle for smooth data weighting should be added to the 180° rotation, resulting in a minimal rotation of approximately 260° for image reconstruction.<sup>13</sup> The influence of the fan angle increases if the positioning of the heart deviates from the centre of the scan field, resulting in lower temporal resolution. The maximal tube rotation speed of current scanners is within the range of 250–350 ms (Table 2). Additional hardware-based

0 Figure 6. Step-by-step strategies to optimize image quality and radiation dose with coronary CT angiography (CTA): different 59  
 1 actions can be implemented to produce sizable effects towards image quality and radiation dose optimization with current 60  
 2 coronary CTA technology. The grey boxes highlight the role of expected technological advances. BMI, body mass index; BP, blood 61  
 3 pressure; HR, heart rate; IR, iterative reconstruction; kV, kilovoltage; mA, milliamperere. 62



49 improvements of temporal resolution have been made possible  
 50 with DSCT. DSCT is constructed with two X-ray tubes at an  
 51 angle of approximately 90°, and two corresponding detector  
 52 rows within a single gantry, resulting in a twofold increased  
 53 temporal resolution in comparison with single-source scanners.

54  
 55 Scanner tubes have benefited from flying focal spot technologies,  
 56 along with improved power and cooling capacities. Emphasis on  
 57 detector properties has led to increased sensitivity to photons,  
 58 along with reduced collimation and reduced refractory period

108 between detected pulses. Since spatial resolution of multi-  
 109 detector CT is influenced by collimation and focal spot size,<sup>13</sup> it  
 110 has especially improved since the introduction of submillimetre  
 111 (0.5–0.625 mm) detector size elements. Recent detector tech-  
 112 nologies, along with tube energy rapid switching capacity and  
 113 dual source in some vendors, have made dual-energy scanning  
 114 possible, which allows assessment of the X-ray absorption  
 115 spectra from a broad range of monoenergetic exposure. Re-  
 116 garding image quality, dual-energy acquisitions allow the re-  
 117 construction of the anatomy at both a low (virtual) and high

energy (kiloelectron volt),<sup>33</sup> which may be helpful to mitigate streak artefacts or assess tissue iodine concentration.

Increased detector coverage to 8 cm and 16 cm per gantry rotation using 256- and 320-row detector scanners, respectively, currently enables heart coverage with minimal or even no table movement. Image acquisition time is shortened, requiring a minimal number of heartbeats (ideally one) and a shorter breath-hold, with less susceptibility to the occurrence of arrhythmias or ectopic beats. An alternative approach for obtaining single heart beat coverage is by using fast table movement (high-pitch) spiral acquisition protocols, currently only possible with DSCT systems.<sup>34</sup>

**Software solutions**

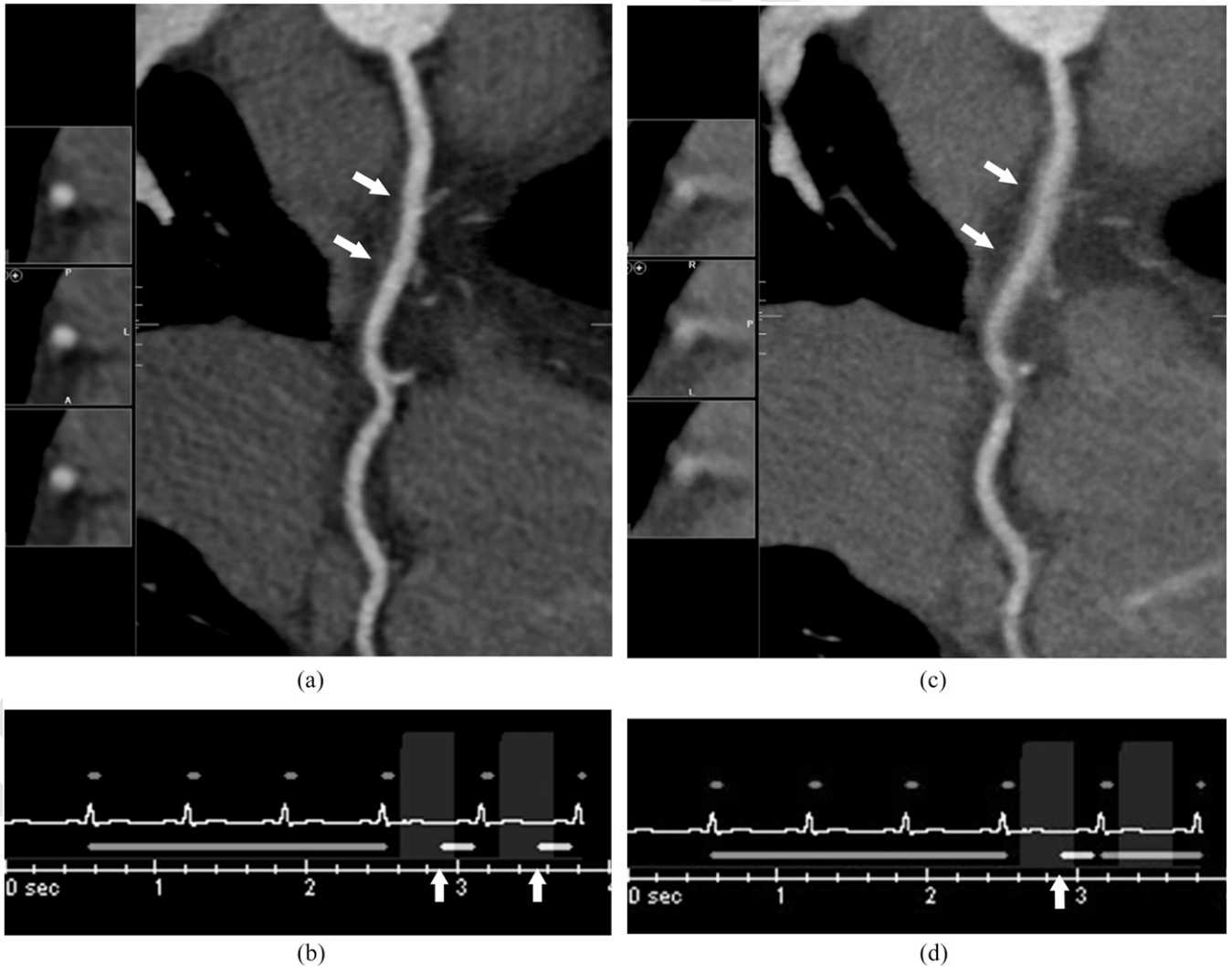
One of the specific challenges of coronary CTA is correcting ECG synchronization of the data acquisition to the HR of the patient. ECG synchronization can be either prospective or

retrospective. With retrospective ECG-gated techniques, scanning is performed throughout the entire cardiac cycle. After all data have been obtained, a user-defined reconstruction of the desired segments of the cardiac cycle is performed, corresponding to the optimal phase of the coronary arteries with least coronary motion. Conversely, in prospective ECG triggering, scanning is only performed during a predefined segment of the cardiac cycle, typically at end diastole in lower and stable HRs.

Temporal resolution is further influenced by the choice between monosegment and multisegment reconstruction (Figure 7). The monosegment reconstruction mode is typically applied in HR <65–75 bpm, the upper limit depending on the effective temporal resolution (gantry rotation time) of the available equipment. When used in higher HR, the delivered temporal resolution is insufficient to provide high-quality images. In such instances, multisegment reconstruction is typically used to improve the temporal resolution. In multisegment acquisitions,

Figure 7. Coronary CT angiography in a 41-year-old male with a heart rate of 92 bpm: excellent image quality (arrows in a) of the right coronary artery is obtained on the long-axis curvilinear and orthogonal reformations after multisegment reconstruction of whole-heart data acquired over two cardiac cycles (arrows in b). The reconstruction of singlesegment data (arrow in d) resulted in a lower temporal resolution and caused a poorer image quality (arrows in c).

ONLINE COLOR ONLY





several partial scans at a given position are acquired, multiplying the temporal resolution by a factor equal to the number of segments. Contrary to monosegment reconstructions, at least two heartbeats are needed, which can be acquired prospectively or retrospectively. Multisegment data acquisition can be applied in a prospective triggering mode, if the detector array is large enough to cover a substantial part of the cardiac volume per rotation. In retrospective ECG-gated acquisitions, multisegment reconstructions require a smaller pitch for similar HRs than monosegment reconstructions to provide sufficient data redundancy with regard to the actual HR.<sup>3,35</sup> Disadvantages of multisegment reconstructions include the requirement that all segment imaging should be performed within exactly the same phase of the cardiac cycle, and spatially adjacent segments have to be imaged in the same cardiac phase to build-up smooth half-scan intervals. Unfortunately, variations in consecutive cardiac cycles tend to increasingly lower image quality using multisegment reconstruction as compared with monosegment. Moreover, in retrospective gated acquisitions, there is a complex relationship between the

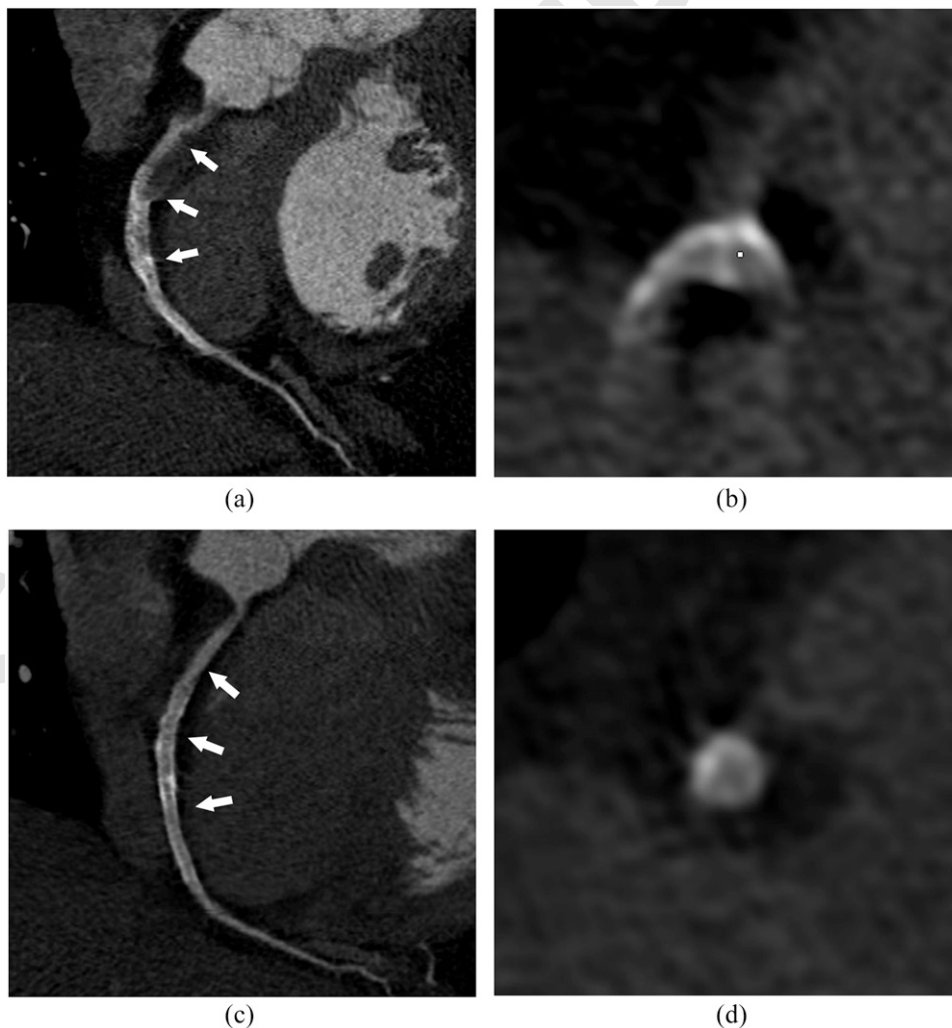
cardiac cycle duration (HR), the rotation speed and multisegment reconstruction.<sup>36,37</sup>

Other recently introduced motion-reducing software algorithms include automated boundary detection and algorithms using information from adjacent cardiac phases within a single cardiac cycle to characterize vessel motion (Figure 8). As such, actual vessel position is determined at the target phase and adaptively compensated to reduce unexpected motion.<sup>38</sup>

Strategies to tackle arrhythmia depend on the type of acquisition: (i) for retrospective spiral acquisitions, arrhythmia-induced artefacts can be countered with retrospective editing of the reconstruction phases based on the continuous ECG registration during the acquisition; (ii) for prospective and high-pitch spiral scans, the acquisition is automatically suspended and delayed to a following heartbeat when HR changes are detected.<sup>37</sup>

The in-plane spatial resolution of CT theoretically approximates the 0.1 mm and 0.2 mm spatial resolution of intravascular

Figure 8. Long- and short-axis multiplanar reformats of the right coronary artery on a prospective electrocardiogram-triggered acquisition with an average heart rate of 67 bpm without (a and b) and with a temporal resolution improvement algorithm (c and d), allowing minimization of the cardiac motion-related blurring on the right coronary artery and assessment of the stent patency (arrows in a and c).



ultrasound and catheter angiography, respectively. However, in clinical practice, the in-plane spatial resolution is limited to approximately 0.5 mm by the use of smoothing convolution reconstruction algorithms. Although such a spatial resolution is sufficient for the assessment of significant coronary artery stenosis in vessels of 1.5 mm or more in diameter, it may remain inadequate to assess stent patency and to confidently grade coronary stenosis in severely calcified arteries.<sup>39,40</sup>

In order to achieve a spatial resolution comparable with catheter angiography, theoretically a 16-fold increase of the radiation dose would be needed, since an increase of spatial resolution proportionally increases image noise in standard filtered back projection (FBP) reconstructions.<sup>13</sup> Recently implemented noise reduction reconstruction algorithms, the so-called iterative reconstruction, in combination with dedicated sharp reconstruction algorithms, theoretically allow decoupling of spatial resolution and image noise for better image quality and improved diagnostic performance for the evaluation of in-stent lumen (Figure 9) and coronary calcifications by reducing partial volume effects.<sup>41,42</sup>

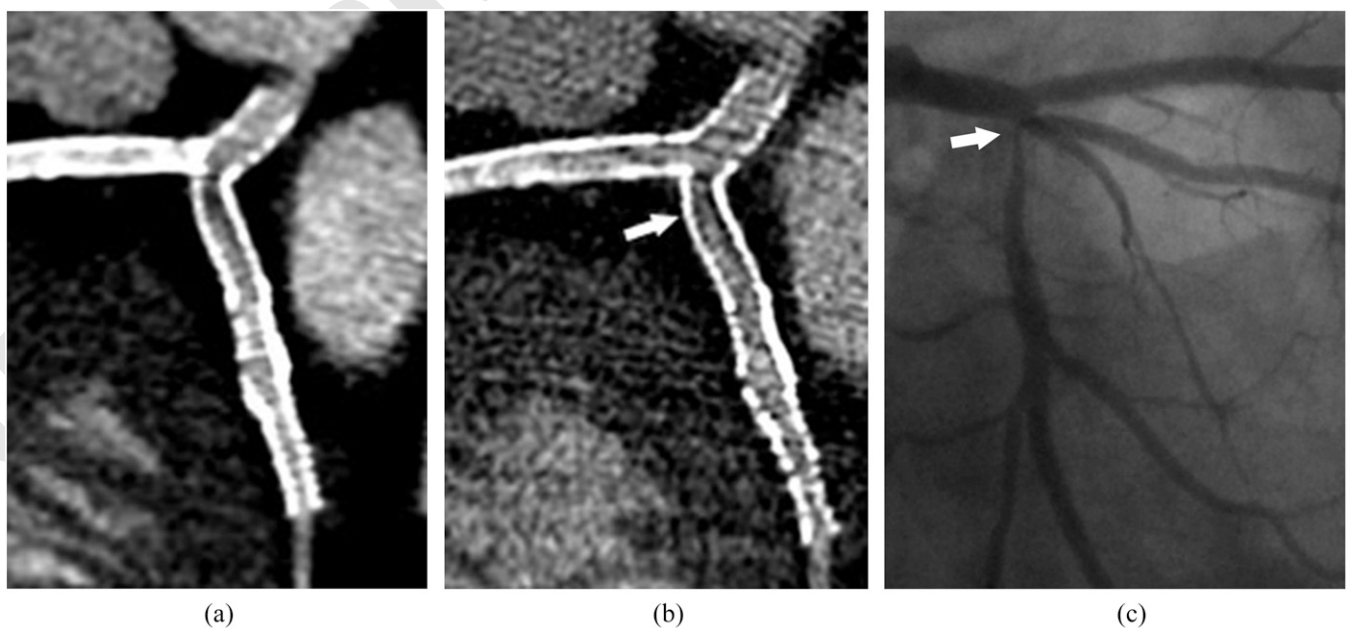
### RADIATION EXPOSURE SAVING AND TRADE-OFFS

Initially, coronary CTA was typically associated with radiation doses amongst the highest in medical imaging, with reported  $E$  ranging up to 16–32 mSv.<sup>43</sup> Today, radiation exposure has been drastically reduced by technical advances and the implementation of dose-efficient strategies, while maintaining high-quality images.<sup>44</sup> Standard dose reduction strategies are: (i) dynamic tube current modulation by cardiac phase and tissue density, (ii) tube voltage reduction and (iii) dynamic collimation in helical

acquisition. One study reported a dose reduction of 68% by shifting from retrospective to prospective ECG modulation in patients with a low and stable HR (mean 56 bpm) and a 53% dose reduction by switching the tube voltage from 120 kV to 100 kV.<sup>45,46</sup> The limitations of tube voltage reduction are increased image noise levels and tube heating. It should therefore be primarily considered in patients who are not obese (BMI <30 kg m<sup>-2</sup>). Dynamic collimation helps to reduce undesired exposure due to z-axis overbeaming, which is particularly prominent with helical scanning (24% dose saving).<sup>47</sup> More recent strategies to reduce dose are the above-discussed high-pitch DSCT acquisition, wide coverage scanners and iterative reconstruction. Compared with standard FBP, hybrid iterative reconstruction refers to an algorithm using mathematical and statistical modelling to reduce image noise while trying to preserve high-resolution images by performing repeated backward “iterative” reconstruction cycles, resulting in a reduction of exposure without increase of noise.<sup>42,48</sup> Although all manufacturers now employ at least one hybrid iterative reconstruction algorithm technology, the implementation and performance of these systems can vary significantly.<sup>42,49</sup> Further newer systems using full-iterative reconstruction are progressively being implemented. Obviously, the largest dose reductions can be achieved by a combination of previously described strategies.<sup>12,34</sup>

Despite the fact that nowadays the  $E$  in coronary CTA can approach the level of annual background radiation under certain conditions, the female breast tissue dose remains a concern and is reported 10–30 times higher<sup>50</sup> compared with the achievable dose of 2.0 mGy in standard mammography for standard breast thickness.<sup>51</sup>

Figure 9. Coronary CT angiography in a 55-year-old male with history of left main trunk, left anterior descending and circumflex artery stenting: two different reconstructions algorithms (standard in a and sharper in b) are performed using iterative reconstruction techniques and the smallest field of view (8 cm). With the sharper reconstruction algorithm, higher image noise is seen as compared with the standard reconstruction, but more details of the proximal circumflex artery severe in-stent restenosis are seen (arrow in b), with a better correlation with catheter coronary angiography (arrow in c).



Besides implementing the earlier described dose-efficient scan modes, further breast dose reduction can be achieved by selective in-plane bismuth shielding. Although controversy still exists regarding its use owing to the deleterious impact on image noise, studies do report 40–50% breast dose savings.<sup>52</sup> Moreover, a recent study reported a degradation of the image quality and no effect on the amount of DNA damage using breast shielding during coronary CTA in females.<sup>53</sup>

## IMAGE QUALITY AND FUTURE DIRECTIONS

Further improvements in scanner hardware, software and image processing are promising for a better image quality and/or less radiation dose (Figure 9).

Coronary motion will be further reduced by intelligent motion correction algorithms, faster transfer systems and multisource scanning,<sup>38,54</sup> whose implementation, alone or in combination, is currently limited by the computational demand in image reconstruction power.

Conversely, advances in spectral imaging have paved the way towards photon counting, a technology in which the whole photonic spectrum is analyzed.<sup>55</sup> However, it is currently not clinically implemented as the limited count rate, energy-integrating detection, increased detector pixel crosstalk and electronic noise are major limitations of this technology.<sup>56</sup> Eventually, photon counting is expected to improve soft-tissue discrimination, to reduce the radiation dose and to provide higher spatial resolution.<sup>57</sup> Compared with dual energy, photon-counting coronary CTA will provide more detailed information about myocardial and coronary plaque components by analyzing differences in contrast agent concentration and/or spectral attenuation.

In addition, improvement of spatial resolution is expected from ongoing development of detector technology, which could provide a reduction of the slice collimation without significant increase of the radiation exposure. This can currently only be achieved at the cost of increasing noise.<sup>58</sup>

In contrast to hybrid iterative reconstruction algorithms, full-iterative algorithms introduce model-based forward projection reconstruction analyses, resulting in a further decoupling between the image noise and radiation dose, especially in the low-dose ranges (volume CT dose index 2–4 mGy). >50% noise suppression is reported compared with the standard FBP. Disadvantages of full-iterative reconstruction algorithms are the computational demands, resulting in substantially longer image reconstruction times.<sup>59–63</sup>

## CONCLUSION

The recent vendor-specific advances have resulted in a dramatic improvement of scanning coverage, spatial, temporal and contrast resolution. Easier acquisition, post-processing and better diagnostic confidence are expected from the ongoing image quality improvement. In parallel, patient safety has been improved by dose reduction strategies and recent achievements indicate that even further dose reductions are to be expected in the near future. There are similarities, but also marked differences between main CT constructor technologies. It is therefore questionable how far a combination of the main strengths from each constructor into one single “perfect” scanner would not represent a huge step. Meanwhile, the current state-of-the-art scanners have already shifted the perception of coronary CTA being a harmful technique towards a dose-efficient technique that is associated with only minor radiation exposure, paving the way for newer indications such as coronary and cardiac tissue composition imaging.

## REFERENCES

- Raff GL. Interpreting the evidence: how accurate is coronary computed tomography angiography? *J Cardiovasc Comput Tomogr* 2007; **1**: 73–7. doi: <https://doi.org/10.1016/j.jcct.2007.04.014>
- Kroft LJ, de Roos A, Geleijns J. Artifacts in ECG-synchronized MDCT coronary angiography. *AJR Am J Roentgenol* 2007; **189**: 581–91. doi: <https://doi.org/10.2214/AJR.07.2138>
- Mahesh M, Cody DD. Physics of cardiac imaging with multiple-row detector CT. *Radiographics* 2007; **27**: 1495–509. doi: <https://doi.org/10.1148/rg.275075045>
- Ghekiere O, Nchimi A, Djekic J, El Hachemi M, Mancini I, Hansen D, et al. Coronary computed tomography angiography: patient-related factors determining image quality using a second-generation 320-slice CT scanner. *Int J Cardiol* 2016; **221**: 970–6. doi: <https://doi.org/10.1016/j.ijcard.2016.07.141>
- Toth T. *Radiation dose from multidetector CT*. 2nd edn. Berlin, Germany: Springer-Verlag; 2012.
- Tatsugami F, Higaki T, Nakamura Y, Yamagami T, Date S, Fujioka C, et al. A new technique for noise reduction at coronary CT angiography with multi-phase data-averaging and non-rigid image registration. *Eur Radiol* 2015; **25**: 41–8. doi: <https://doi.org/10.1007/s00330-014-3381-9>
- Leschka S, Stolzmann P, Schmid FT, Scheffel H, Stinn B, Marincek B, et al. Low kilovoltage cardiac dual-source CT: attenuation, noise, and radiation dose. *Eur Radiol* 2008; **18**: 1809–17. doi: <https://doi.org/10.1007/s00330-008-0966-1>
- Tatsugami F, Matsuki M, Nakai G, Inada Y, Kanazawa S, Takeda Y, et al. The effect of adaptive iterative dose reduction on image quality in 320-detector row CT coronary angiography. *Br J Radiol* 2012; **85**: e378–82. doi: <https://doi.org/10.1259/bjr/10084599>
- Achenbach S, Paul JF, Laurent F, Becker HC, Rengo M, Caudron J, et al. Comparative assessment of image quality for coronary CT angiography with iobitridol and two contrast agents with higher iodine concentrations: iopromide and iomeprol. A multicentre randomized double-blind trial. *Eur Radiol* 2016; **27**: 821–30. doi: <https://doi.org/10.1007/s00330-016-4437-9>
- Kim EY, Yeh DW, Choe YH, Lee WJ, Lim HK. Image quality and attenuation values of multidetector CT coronary angiography using high iodine-concentration contrast material: a comparison of the use of iopromide 370 and iomeprol 400. *Acta Radiol* 2010; **51**: 982–9. doi: <https://doi.org/10.3109/02841851.2010.509740>
- Odedra D, Blobel J, Alhumayyd S, Durand M, Jimenez-Juan L, Paul N. Image noise-based

- dose adaptation in dynamic volume CT of the heart: dose and image quality optimisation in comparison with BMI-based dose adaptation. *Eur Radiol* 2014; **24**: 86–94. doi: <https://doi.org/10.1007/s00330-013-2980-1>
12. Chen MY, Shanbhag SM, Arai AE. Submillisievert median radiation dose for coronary angiography with a second-generation 320-detector row CT scanner in 107 consecutive patients. *Radiology* 2013; **267**: 76–85. doi: <https://doi.org/10.1148/radiol.13122621>
13. Flohr TG, Raupach R, Bruder H. Cardiac CT: how much can temporal resolution, spatial resolution, and volume coverage be improved? *J Cardiovasc Comput Tomogr* 2009; **3**: 143–52. doi: <https://doi.org/10.1016/j.jcct.2009.04.004>
14. Geleijns J. Physics background and radiation exposure. In: Dewey M, ed. *Cardiac CT*. 2nd edn. Heidelberg, Germany: Springer; 2013. pp. 57–70.
15. Huda W, Tipnis S, Sterzik A, Schoepf UJ. Computing effective dose in cardiac CT. *Phys Med Biol* 2010; **55**: 3675–84. doi: <https://doi.org/10.1088/0031-9155/55/13/007>
16. Deak P, van Straten M, Shrimpton PC, Zankl M, Kalender WA. Validation of a Monte Carlo tool for patient-specific dose simulations in multi-slice computed tomography. *Eur Radiol* 2008; **18**: 759–72. doi: <https://doi.org/10.1007/s00330-007-0815-7>
17. Martin CJ. Effective dose: how should it be applied to medical exposures? *Br J Radiol* 2007; **80**: 639–47. doi: <https://doi.org/10.1259/bjr/25922439>
18. Maintz D, Seifarth H, Raupach R, Flohr T, Rink M, Sommer T, et al. 64-slice multi-detector coronary CT angiography: *in vitro* evaluation of 68 different stents. *Eur Radiol* 2006; **16**: 818–26. doi: <https://doi.org/10.1007/s00330-005-0062-8>
19. Maintz D, Burg MC, Seifarth H, Bunck AC, Ozgun M, Fischbach R, et al. Update on multidetector coronary CT angiography of coronary stents: *in vitro* evaluation of 29 different stent types with dual-source CT. *Eur Radiol* 2009; **19**: 42–9. doi: <https://doi.org/10.1007/s00330-008-1132-5>
20. Bae KT. Intravenous contrast medium administration and scan timing at CT: considerations and approaches. *Radiology* 2010; **256**: 32–61. doi: <https://doi.org/10.1148/radiol.10090908>
21. Leiner T, Abbara S. Contrast injection protocols: it is time to get creative! *J Cardiovasc Comput Tomogr* 2015; **9**: 28–30. doi: <https://doi.org/10.1016/j.jcct.2015.01.006>
22. Blankstein R, Bolen MA, Pale R, Murphy MK, Shah AB, Bezerra HG, et al. Use of 100 kV versus 120 kV in cardiac dual source computed tomography: effect on radiation dose and image quality. *Int J Cardiovasc Imaging* 2011; **27**: 579–86. doi: <https://doi.org/10.1007/s10554-010-9683-3>
23. Gill MK, Vijayanathan A, Kumar G, Jayarani K, Ng KH, Sun Z. Use of 100 kV versus 120 kV in computed tomography pulmonary angiography in the detection of pulmonary embolism: effect on radiation dose and image quality. *Quant Imaging Med Surg* 2015; **5**: 524–33.
24. Ippolito D, Talei Franzesi C, Fior D, Bonaffini PA, Minutolo O, Sironi S. Low kV settings CT angiography (CTA) with low dose contrast medium volume protocol in the assessment of thoracic and abdominal aorta disease: a feasibility study. *Br J Radiol* 2015; **88**: 20140140. doi: <https://doi.org/10.1259/bjr.20140140>
25. Oda S, Utsunomiya D, Yuki H, Kai N, Hatemura M, Funama Y, et al. Low contrast and radiation dose coronary CT angiography using a 320-row system and a refined contrast injection and timing method. *J Cardiovasc Comput Tomogr* 2015; **9**: 19–27. doi: <https://doi.org/10.1016/j.jcct.2014.12.002>
26. Vavere AL, Arbab-Zadeh A, Rochitte CE, Dewey M, Niinuma H, Gottlieb I, et al. Coronary artery stenoses: accuracy of 64-detector row CT angiography in segments with mild, moderate, or severe calcification—a subanalysis of the CORE-64 trial. *Radiology* 2011; **261**: 100–8. doi: <https://doi.org/10.1148/radiol.11110537>
27. Abdulla J, Pedersen KS, Budoff M, Kofoed KF. Influence of coronary calcification on the diagnostic accuracy of 64-slice computed tomography coronary angiography: a systematic review and meta-analysis. *Int J Cardiovasc Imaging* 2012; **28**: 943–53. doi: <https://doi.org/10.1007/s10554-011-9902-6>
28. den Dekker MA, de Smet K, de Bock GH, Tio RA, Oudkerk M, Vliegenthart R. Diagnostic performance of coronary CT angiography for stenosis detection according to calcium score: systematic review and meta-analysis. *Eur Radiol* 2012; **22**: 2688–98. doi: <https://doi.org/10.1007/s00330-012-2551-x>
29. Shapiro MD, Pena AJ, Nichols JH, Worrell S, Bamberg F, Dannemann N, et al. Efficacy of pre-scan beta-blockade and impact of heart rate on image quality in patients undergoing coronary multidetector computed tomography angiography. *Eur J Radiol* 2008; **66**: 37–41. doi: <https://doi.org/10.1016/j.ejrad.2007.05.006>
30. Celik O, Atasoy MM, Erturk M, Yalcin AA, Aksu HU, Diker M, et al. Comparison of different strategies of ivabradine pre-medication for heart rate reduction before coronary computed tomography angiography. *J Cardiovasc Comput Tomogr* 2014; **8**: 77–82. doi: <https://doi.org/10.1016/j.jcct.2013.12.005>
31. Takx RA, Sucha D, Park J, Leiner T, Hoffmann U. Sublingual nitroglycerin administration in coronary computed tomography angiography: a systematic review. *Eur Radiol* 2015; **25**: 3536–42. doi: <https://doi.org/10.1007/s00330-015-3791-3>
32. Muenzel D, Noel PB, Dorn F, Dobritz M, Rummeny EJ, Huber A. Step and shoot coronary CT angiography using 256-slice CT: effect of heart rate and heart rate variability on image quality. *Eur Radiol* 2011; **21**: 2277–84. doi: <https://doi.org/10.1007/s00330-011-2185-4>
33. Johnson TR. Dual-energy CT: general principles. *AJR Am J Roentgenol* 2012; **199**: S3–8. doi: <https://doi.org/10.2214/AJR.12.9116>
34. Schuhbaeck A, Achenbach S, Layritz C, Eisentopf J, Hecker F, Pflederer T, et al. Image quality of ultra-low radiation exposure coronary CT angiography with an effective dose <0.1 mSv using high-pitch spiral acquisition and raw data-based iterative reconstruction. *Eur Radiol* 2013; **23**: 597–606. doi: <https://doi.org/10.1007/s00330-012-2656-2>
35. Tomizawa N, Komatsu S, Akahane M, Torigoe R, Kiryu S, Ohtomo K. Relationship between beat to beat coronary artery motion and image quality in prospectively ECG-gated two heart beat 320-detector row coronary CT angiography. *Int J Cardiovasc Imaging* 2012; **28**: 139–46. doi: <https://doi.org/10.1007/s10554-010-9759-0>
36. Hein PA, May J, Rogalla P, Butler C, Hamm B, Lembcke A. Feasibility of contrast material volume reduction in coronary artery imaging using 320-slice volume CT. *Eur Radiol* 2010; **20**: 1337–43. doi: <https://doi.org/10.1007/s00330-009-1692-z>
37. Lesser JR, Flygenring BJ, Knickelbine T, Longe T, Schwartz RS. Practical approaches to overcoming artifacts in coronary CT angiography. *J Cardiovasc Comput Tomogr* 2009; **3**: 4–15. doi: <https://doi.org/10.1016/j.jcct.2008.11.006>
38. Leipsic J, Labounty TM, Hague CJ, Mancini GB, O'Brien JM, Wood DA, et al. Effect of a novel vendor-specific motion-correction algorithm on image quality and diagnostic accuracy in persons undergoing coronary CT angiography without rate-control medications. *J Cardiovasc Comput Tomogr* 2012; **6**: 164–71. doi: <https://doi.org/10.1016/j.jcct.2012.04.004>
39. Hou Y, Ma Y, Fan W, Wang Y, Yu M, Vembar M, et al. Diagnostic accuracy of low-dose 256-slice multi-detector coronary CT angiography using iterative reconstruction in patients with suspected coronary artery

- disease. *Eur Radiol* 2014; **24**: 3–11. doi: <https://doi.org/10.1007/s00330-013-2969-9>
40. Gebhard C, Fiechter M, Fuchs TA, Stehli J, Muller E, Stahl BE, et al. Coronary artery stents: influence of adaptive statistical iterative reconstruction on image quality using 64-HDCT. *Eur Heart J Cardiovasc Imaging* 2013; **14**: 969–77. doi: <https://doi.org/10.1093/ehjci/etj013>
41. Ebersberger U, Tricarico F, Schoepf UJ, Blanke P, Spears JR, Rowe GW, et al. CT evaluation of coronary artery stents with iterative image reconstruction: improvements in image quality and potential for radiation dose reduction. *Eur Radiol* 2013; **23**: 125–32. doi: <https://doi.org/10.1007/s00330-012-2580-5>
42. Willeminck MJ, de Jong PA, Leiner T, de Heer LM, Nievelstein RA, Budde RP, et al. Iterative reconstruction techniques for computed tomography Part 1: technical principles. *Eur Radiol* 2013; **23**: 1623–31. doi: <https://doi.org/10.1007/s00330-012-2765-y>
43. Mettler FA Jr, Huda W, Yoshizumi TT, Mahesh M. Effective doses in radiology and diagnostic nuclear medicine: a catalog. *Radiology* 2008; **248**: 254–63. doi: <https://doi.org/10.1148/radiol.2481071451>
44. Cademartiri F, Maffei E, Arcadi T, Catalano O, Midiri M. CT coronary angiography at an ultra-low radiation dose (<0.1 mSv): feasible and viable in times of constraint on health-care costs. *Eur Radiol* 2013; **23**: 607–13. doi: <https://doi.org/10.1007/s00330-012-2767-9>
45. Bischoff B, Hein F, Meyer T, Hadamitzky M, Martinoff S, Schomig A, et al. Impact of a reduced tube voltage on CT angiography and radiation dose: results of the PROTECTION I study. *JACC Cardiovasc Imaging* 2009; **2**: 940–6. doi: <https://doi.org/10.1016/j.jcmg.2009.02.015>
46. Bischoff B, Hein F, Meyer T, Krebs M, Hadamitzky M, Martinoff S, et al. Comparison of sequential and helical scanning for radiation dose and image quality: results of the prospective multicenter study on radiation dose estimates of cardiac CT angiography (PROTECTION) I study. *AJR Am J Roentgenol* 2010; **194**: 1495–9. doi: <https://doi.org/10.2214/AJR.09.3543>
47. Walker MJ, Desai MY, Halliburton SS, Flamm SD. New radiation dose saving technologies for 256-slice cardiac computed tomography angiography. *Int J Cardiovasc Imaging* 2009; **25**: 189–99. doi: <https://doi.org/10.1007/s10554-009-9444-3>
48. Wang R, Schoepf UJ, Wu R, Reddy RP, Zhang C, Yu W, et al. Image quality and radiation dose of low dose coronary CT angiography in obese patients: sinogram affirmed iterative reconstruction versus filtered back projection. *Eur J Radiol* 2012; **81**: 3141–5. doi: <https://doi.org/10.1016/j.ejrad.2012.04.012>
49. Mievilte FA, Gudinchet F, Brunelle F, Bochud FO, Verdun FR. Iterative reconstruction methods in two different MDCT scanners: physical metrics and 4-alternative forced-choice detectability experiments—a phantom approach. *Phys Med* 2013; **29**: 99–110.
50. Einstein AJ, Elliston CD, Arai AE, Chen MY, Mather R, Pearson GD, et al. Radiation dose from single-heartbeat coronary CT angiography performed with a 320-detector row volume scanner. *Radiology* 2010; **254**: 698–706. doi: <https://doi.org/10.1148/radiol.09090779>
51. Perry NB, Wolf C, Törnberg S, Holland R, von Karsa L. *European guidelines for quality assurance in breast cancer screening and diagnosis*. 4th edn. Luxembourg: European Communities; 2013.
52. Abadi S, Mehrez H, Ursani A, Parker M, Paul N. Direct quantification of breast dose during coronary CT angiography and evaluation of dose reduction strategies. *AJR Am J Roentgenol* 2011; **196**: W152–8. doi: <https://doi.org/10.2214/AJR.10.4626>
53. Cheezum MK, Redon CE, Burrell AS, Kaviratne AS, Bindeman J, Maeda D, et al. Effects of breast shielding during heart imaging on DNA double-strand-break levels: a prospective randomized controlled trial. *Radiology* 2016; **281**: 62–71. doi: <https://doi.org/10.1148/radiol.2016152301>
54. Wang G, Yu H, Ye Y. A scheme for multisource interior tomography. *Med Phys* 2009; **36**: 3575–81. doi: <https://doi.org/10.1118/1.3157103>
55. de Vries A, Roessl E, Kneepkens E, Thran A, Brendel B, Martens G, et al. Quantitative spectral K-edge imaging in preclinical photon-counting X-ray computed tomography. *Invest Radiol* 2015; **50**: 297–304. doi: <https://doi.org/10.1097/RLI.0000000000000126>
56. Yu Z, Leng S, Jorgensen SM, Li Z, Gutjahr R, Chen B, et al. Evaluation of conventional imaging performance in a research whole-body CT system with a photon-counting detector array. *Phys Med Biol* 2016; **61**: 1572–95. doi: <https://doi.org/10.1088/0031-9155/61/4/1572>
57. Boussel L, Coulon P, Thran A, Roessl E, Martens G, Sigovan M, et al. Photon counting spectral CT component analysis of coronary artery atherosclerotic plaque samples. *Br J Radiol* 2014; **87**: 20130798. doi: <https://doi.org/10.1259/bjr.20130798>
58. Pelc NJ. Recent and future directions in CT imaging. *Ann Biomed Eng* 2014; **42**: 260–8. doi: <https://doi.org/10.1007/s10439-014-0974-z>
59. Nishiyama Y, Tada K, Mori H, Maruyama M, Katsube T, Yamamoto N, et al. Effect of the forward-projected model-based iterative reconstruction solution algorithm on image quality and radiation dose in pediatric cardiac computed tomography. *Pediatr Radiol* 2016; **46**: 1663–70. doi: <https://doi.org/10.1007/s00247-016-3676-x>
60. Sucha D, Willeminck MJ, de Jong PA, Schilham AM, Leiner T, Symersky P, et al. The impact of a new model-based iterative reconstruction algorithm on prosthetic heart valve related artifacts at reduced radiation dose MDCT. *Int J Cardiovasc Imaging* 2014; **30**: 785–93.
61. Stehli J, Fuchs TA, Bull S, Clerc OF, Possner M, Buechel RR, et al. Accuracy of coronary CT angiography using a submillisievert fraction of radiation exposure: comparison with invasive coronary angiography. *J Am Coll Cardiol* 2014; **64**: 772–80. doi: <https://doi.org/10.1016/j.jacc.2014.04.079>
62. Wang W, Ionita C, Huang Y, Qu B, Panse A, Jain A, et al. Region-of-interest microangiographic fluoroscope detector used in aneurysm and artery stenosis diagnoses and treatment. *Proc SPIE Int Soc Opt Eng* 2012; **23**: 8313. doi: <https://doi.org/10.1117/12.910771>
63. den Harder AM, Willeminck MJ, de Jong PA, Schilham AM, Rajiah P, Takx RA, et al. New horizons in cardiac CT. *Clin Radiol* 2016; **71**: 758–67. doi: <https://doi.org/10.1016/j.crad.2016.01.022>

## PROOFS

The British Journal of Radiology  
48–50 St John Street  
London EC1M 4DG, UK  
Tel: +44 (0)20 3668 2220  
E-mail: [BJRproduction@bir.org.uk](mailto:BJRproduction@bir.org.uk)

Dear Author,

Please find enclosed a proof of your article "**Image quality in coronary CT angiography: challenges and technical solutions**" for checking.

When reading through your proof, please check carefully authors' names, scientific data, data in tables, any mathematics, units and the accuracy of references. Please note that only typographical errors and data corrections are allowed at this stage. Corrections can be returned by annotating the PDF, in a Word document or in e-mail text. Please ensure that all queries are addressed.

Please also check the quality of the figures. For information about electronic image preparation, see the instructions for authors (<http://www.birpublications.org/page/ifa/bjr>)

Any queries that have arisen during preparation of your paper for publication are listed below and indicated on the proof. Please provide your answers when returning your proof.

Please return your proof by e-mail within 2 days of receipt.

Query no.	Page no.	Query
1	1	Please check the preferred title (Dr) included for the corresponding author in the correspondence line.
2	2	Please clarify whether the phrase "then obtained standard deviation" could be changed to "then-obtained standard deviation" in the sentence "The then obtained standard ...".
3	3	Please consider providing the unit of measurement for the matrix value given in the sentence "It is determined by the matrix ...".
4	3	Please spell out "CCTA" in text.
5	4	Please check whether the edits made to the sentence "In blooming artefacts ..." are correct.
6	3	Please verify the significance of colour with regard to Figures 1, 2, 5 and 7 because this article is being printed in black and white and is in colour only online.